

Heavy-Ion Physics

Alejandro Ayala
Instituto de Ciencias Nucleares,
Universidad Nacional Autónoma de México

CERN - Latin-American School of High-Energy Physics
March 2017

Bibliography

- P. Foka and M. A. Janik, *An overview of experimental results from ultra-relativistic heavy-ion collisions at the CERN LHC: Bulk properties and dynamical evolution*, arXiv:1702.07233.
- P. Foka and M. A. Janik, *An overview of experimental results from ultra-relativistic heavy-ion collisions at the CERN LHC: Hard probes*, Reviews in Physics **1** (2016), 172.
- K. Fukushima and T. Hatsuda, *The phase diagram of dense QCD*, Rep. Prog. Phys. **74** (2011) 014001.
- X. Luo and N. Xu, *Search for the QCD critical point with fluctuations of conserved quantities in Relativistic Heavy-Ion Collisions at RHIC: An overview*, arXiv:1701.02105.
- A. Ayala, *Hadronic matter at the edge: A survey of some theoretical approaches to the physics of the QCD phase diagram*, arXiv:1608.04378.
- H. Sazdjian *Introduction to chiral symmetry in QCD*, arXiv:1612.04078.

Contents

- Overview of QCD two main features: chiral symmetry and confinement.
- A survey of the heavy-ion program results: bulk properties and hard probes.
- QCD at finite temperature and density: The phase diagram.
- Phase transitions.
- Search for the critical end point.
- Summary and open questions.

QCD: The theory of strong interactions

- Gauge theory with the **local** symmetry group $SU(N_c)$. (In the real world $N_c = 3$).
- The fundamental fields are the **quarks** (matter fields) and **gluons** gauge fields.
- Each one of the N_f **quark fields** belong to the **fundamental representation** of the color group which is (N_c) -dimensional, **antiquark fields** to the **complex conjugate of the fundamental representation**, also (N_c) -dimensional and **gluon fields** to the adjoint representation which is $(N_c^2 - 1)$ -dimensional.

$$\mathcal{L}_{\text{QCD}} = \sum_{i=1}^{N_f} \bar{\psi}_i^a \left(i\gamma^\mu (\partial_\mu \delta^{ab} + ig_s A_\mu^{ab}) - m_i \delta^{ab} \right) \psi_i^b - \frac{1}{4} G_{\mu\nu}^\alpha G_{\alpha}^{\mu\nu};$$
$$G_{\mu\nu}^\alpha = \partial_\mu A_\nu^\alpha - \partial_\nu A_\mu^\alpha + g_s f^{\alpha\beta\sigma} A_\mu^\beta A_\nu^\sigma; \quad A_\mu^{ab} = A_\mu^\sigma (\tau_\sigma)^{ab}$$

a, b run from 1 to N_c , α, β, σ run from 1 to $N_c^2 - 1$.

Flavor symmetry

- From hadron spectroscopy one deduces that there are several kinds of quarks.
- Quarks are distinguished from one another by a quantum number called **flavor**.
- There are **six flavors**: u, d, s, c, b, t . We refer to the **number of flavors** generically as N_f .
- **Consider the ideal case in which all N_f flavors have the same mass.** Quark and antiquark fields are assigned to the fundamental and complex conjugate representations (each N_f -dimensional), respectively, of the $SU(N_f)$ group.
- The Lagrangian corresponding to the quark sector becomes (we omit color indices for quarks and gluons)

$$\mathcal{L}_q = \sum_{i=1}^N \bar{\psi}_i (i\gamma^\mu (\partial_\mu + ig_s A_\mu) - m) \psi_i$$

Flavor symmetry

- \mathcal{L}_q is invariant under continuous **global transformations** of $SU(N_f)$

$$\begin{aligned}\psi_i &\longrightarrow \psi'_i = e^{-i\alpha^A (T^A)_i^j} \psi_j \\ \bar{\psi}_i &\longrightarrow \bar{\psi}'_i = \bar{\psi}_j e^{i\alpha^A (T^A)^j_i} \\ A_\mu &\longrightarrow A'_\mu = A_\mu; \quad A \text{ runs from } 1 \text{ to } N_f^2 - 1, \\ &\quad T^A \text{ are } N_f \times N_f \text{ matrices}\end{aligned}$$

- In **infinitesimal form**

$$\begin{aligned}\delta\psi_i &= -i\delta\alpha^A (T^A)_i^j \psi_j \\ \delta\bar{\psi}_i &= i\delta\alpha^A \bar{\psi}_j (T^A)^j_i \\ \delta A_\mu &= 0\end{aligned}$$

Flavor symmetry

- Using Noether's theorem, one finds **(exercise)** $N_f^2 - 1$ **conserved currents**

$$\begin{aligned}j_\mu^A(x) &= \bar{\psi}_i(x) \gamma_\mu (T^A)^i_j \psi^j(x) \\ \partial^\mu j_\mu^A &= 0\end{aligned}$$

- The generators of the group **(the charges)** are obtained from j_0^A by space integration

$$Q^A = \int d^3x j_0^A(x)$$

- Q^A 's satisfy the $SU(N_f)$ algebra

$$[Q^A, Q^B] = if^{ABC} Q^C; \quad A, B, C = 1, \dots, N_f^2 - 1$$

Flavor symmetry

- Current conservation implies that **the generators** are independent of time and therefore they **commute with the Hamiltonian** H

$$[H, Q^A] = 0$$

- The transformation properties of the fields can be translated to the states.
- Introduce one-particle quark states (omit spin labels) $|\mathbf{p}, i\rangle$.
- **If the vacuum state is invariant under the group transformations (exercise)**

$$Q^A |\mathbf{p}, i\rangle = (T^A)^j_i |\mathbf{p}, j\rangle$$

Flavor symmetry

- Since these states are also eigenstates of the Hamiltonian, the above means that the various one-particle states of the fundamental representation multiplet have equal masses m

This mode to realize the symmetry is called the **Wigner-Weyl** mode

Approximate flavor symmetry

- Consider the real case where flavors have different masses

$$\mathcal{L}_q = \sum_{i=1}^N \bar{\psi}_i (i\gamma^\mu (\partial_\mu + igA_\mu) - m_i) \psi_i$$

- The mass term spoils $SU(N_f)$ invariance, therefore currents are not conserved and we find (exercise)

$$\partial^\mu j_\mu^A = -i \sum_{i,j=1}^{N_f} (m_i - m_j) \bar{\psi}_i (T^A)^i_j \psi_j \neq 0$$

- In the real world quarks are divided into two groups: **Light quarks** u, d, s and **heavy quarks** c, b, t . The mass difference between each group is large (> 1 GeV). An approximate symmetry can be expected only for light quarks: $SU(2)$ for u, d or $SU(3)$ for u, d, s .

Chiral symmetry

- Quarks can also be transformed by means of unitary transformations that include the γ_5 matrix. The transformations are called **axial flavor transformations**
- In infinitesimal form

$$\begin{aligned}\delta\psi_i &= -i\delta\alpha^A(T^A)_i^j\gamma_5\psi_j \\ \delta\bar{\psi}_i &= i\delta\alpha^A\bar{\psi}_j\gamma_5(T^A)^j_i \\ \delta A_\mu &= 0\end{aligned}$$

- Consider the quark part of the Lagrangian \mathcal{L}_q with equal masses. Under these transformations \mathcal{L}_q **is not invariant because of the mass**

$$\delta\mathcal{L}_q = 2im\delta\alpha^A\bar{\psi}^i(T^A)_i^j\gamma_5\psi_j$$

Chiral symmetry

- Invariance under axial flavor transformations requires vanishing of the quark mass

Contrary to flavor symmetry transformations, equality of masses is not sufficient for invariance under axial flavor transformations

- In the general case of different masses, we introduce the **mass matrix** $\mathcal{M} = \text{diag}(m_1, m_2, \dots, m_{N_f})$
- The variation of the Lagrangian is (exercise)

$$\delta\mathcal{L}_q = i\delta\alpha^A \bar{\psi}^i \{M, T^A\}_i{}^j \gamma_5 \psi_j; \quad \{, \} \text{ is the anticommutator}$$

Chiral symmetry

- Consider the **massless case**. The Lagrangian is invariant under **both** the flavor and the axial flavor transformations. The conserved currents are

$$\begin{aligned}j_{\mu}^A(x) &= \bar{\psi}_i(x) \gamma_{\mu} (T^A)^i_j \psi^j(x); & \partial^{\mu} j_{\mu}^A &= 0 \\j_{5\mu}^A(x) &= \bar{\psi}_i(x) \gamma_{\mu} \gamma_5 (T^A)^i_j \psi^j(x); & \partial^{\mu} j_{5\mu}^A &= 0\end{aligned}$$

- The corresponding charges are

$$Q^A = \int d^3x j_0^A(x), \quad Q_5^A = \int d^3x j_{50}^A(x)$$

Chiral symmetry

- Together the flavor and axial flavor transformations form the **chiral transformations**. The corresponding charges satisfy the commutation relations

$$[Q^A, Q^B] = if^{ABC} Q^C, \quad [Q^A, Q_5^B] = if^{ABC} Q_5^C, \quad [Q_5^A, Q_5^B] = if^{ABC} Q^C$$

- The axial charges do not form an algebra. However, if we define

$$Q_L^A = \frac{1}{2}(Q^A - Q_5^A), \quad Q_R^A = \frac{1}{2}(Q^A + Q_5^A)$$

we obtain (exercise)

$$[Q_L^A, Q_L^B] = if^{ABC} Q_L^C, \quad [Q_R^A, Q_R^B] = if^{ABC} Q_R^C, \quad [Q_L^A, Q_R^B] = 0$$

Chiral symmetry

- The left-handed and right-handed charges decouple and operate separately. Each generate an $SU(N_f)$ group.
- The chiral group is decomposed into the direct product of two $SU(N_f)$ groups, labeled with the subscripts L and R .

$$\text{Chiral group} = SU(N_f)_L \otimes SU(N_f)_R$$

- In the real world, chiral symmetry is not exact, **quark masses break it explicitly.**
- In the light quark sector, the breaking can be treated as a perturbation, the symmetry is approximate.
- **What is the signature of this approximate symmetry?**

Spontaneous chiral symmetry breaking

- Suppose the symmetry is realized in the **Wigner-Weyl mode**.
- **In the massless quark limit** a chiral transformation acting on a massive state gives

$$Q_5^A |M, s, \mathbf{p}, +, i\rangle = (T^A)^j_i |M, s, \mathbf{p}, -, j\rangle$$

- This means that we should find **parity partners** for the massive states. **When we consider the light quark masses, the degeneracy within parity doublets is lifted, but the masses should remain close to each other.**
- No parity doublets are observed, thus the Wigner-Weyl mode realization of chiral symmetry does not happen for **ordinary conditions**.

The alternative is **spontaneous symmetry breaking, also known as Nambu-Goldstone mode**.

Spontaneous chiral symmetry breaking

- What happens if the generators of some transformations do not annihilate the vacuum?

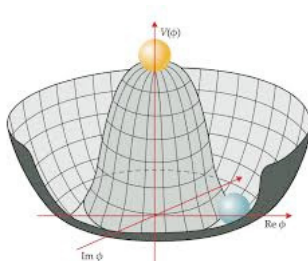
$$Q_5^A |0\rangle \neq 0$$

- In this case we say that **the symmetry has been spontaneously broken.**
- The axial charges when applied to the vacuum state produce new states

$$Q_5^A |0\rangle = |A, -\rangle, \quad A = 1, \dots, N_f^2 - 1$$

- The states have the same properties as the axial charges that generate it, in particular **they are pseudoscalar states.**

Spontaneous chiral symmetry breaking



Goldstone bosons correspond to the directions where the potential is flat

Spontaneous chiral symmetry breaking

- In the massless limit, **the charges commute with the Hamiltonian** therefore, **these states are massless (Goldstone theorem)**.
- **Spontaneous chiral symmetry breaking** is manifested by means of the existence of $N_f^2 - 1$ pseudoscalar massless particles called **Nambu-Goldstone bosons**.
- The breaking of the symmetry involves only the axial sector. The ordinary flavor symmetry is still realized in the Wigner-Weyl mode.

$$SU(N_f)_L \otimes SU(N_f)_R \longrightarrow SU(N_f)_V$$

- In the real world ($N_f = 3$), this corresponds to **eight** pseudoscalar bosons (π, K, η) with small masses (**exercise: how is the parity of a particle measured?**).

Confinement

- Under ordinary circumstances, quarks are **confined within hadrons**.
- Color force characteristics:

- 1 Potential between two quarks at “**long**” distances, $\mathcal{O}(1 \text{ fm})$, is linear.
- 2 Separation of quarks requires “**infinite**” amount of energy.
- 3 **Confinement** is a direct **consequence of gluon self-interaction**.
- 4 Quarks and gluons confined inside QCD potential must combine into zero net color charge particles called **hadrons**.

Coupling constant

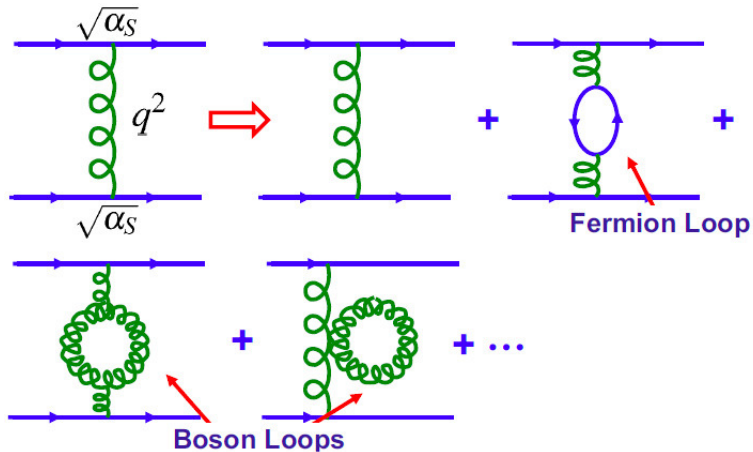
- Strength of strong interaction characterized by coupling “constant”

$$\alpha_s = g_s^2/4\pi.$$

- Coupling constant characteristics:

- 1 Decreases with distance.
- 2 Bare color charge is **antiscreened** due to gluon self-interaction .

Coupling constant



$$Q^2 = -q^2$$

Coupling constant

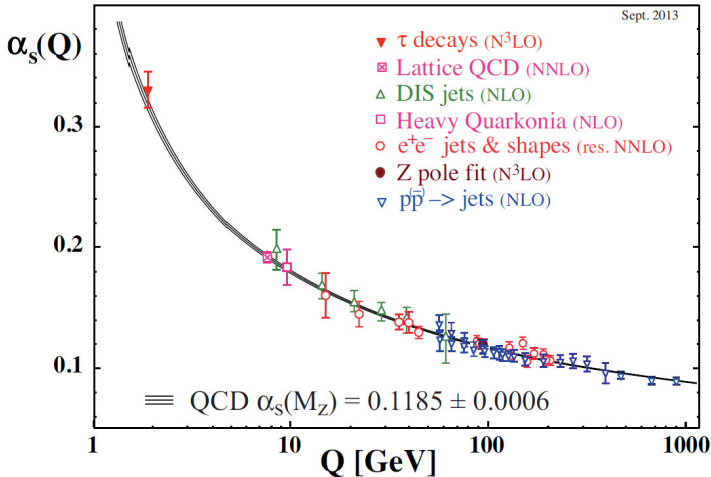
- Competition between color and flavor

$$\alpha_s(Q^2) = \frac{\alpha_s(Q_0^2)}{\left[1 + B\alpha_s(Q_0^2) \ln\left(\frac{Q^2}{Q_0^2}\right)\right]}$$
$$B = \frac{11N_c - 2N_f}{12\pi}$$

$$N_c = 3, \quad N_f = 6 \implies B > 0$$

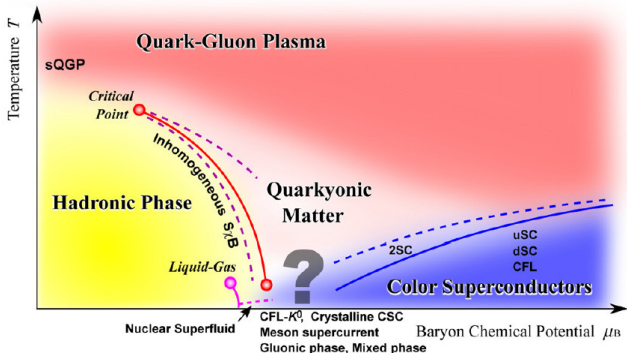
α_s decreases with $Q = \sqrt{Q^2}$

Coupling constant

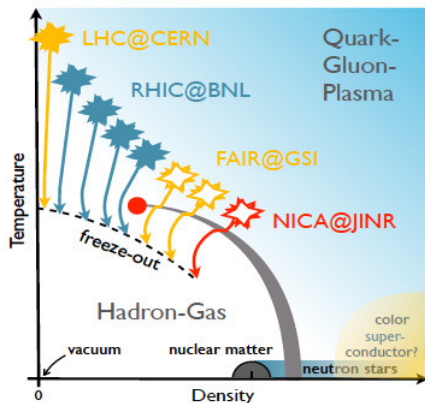


Phase transitions

- Since the coupling constant runs towards smaller values with increasing energy scale **it is natural to anticipate that confined and chiral symmetry broken QCD matter undergoes a phase transition at high energy densities, $T \simeq \Lambda_{QCD} \sim 200$ MeV, $n_B \simeq \Lambda_{QCD}^3 \sim 1 \text{ fm}^{-3}$.**

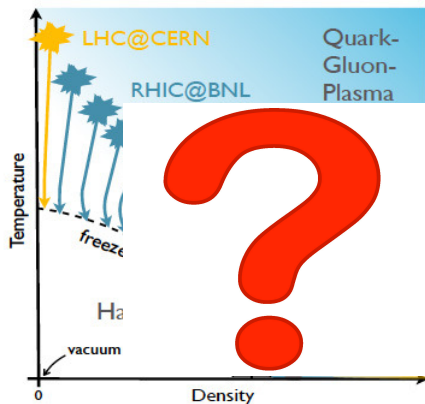


Phase diagram explored with Heavy-Ion collisions



Phase diagram explored with Heavy-Ion collisions

Our current knowledge of the phase diagram is restricted to near the Temperature-axis.



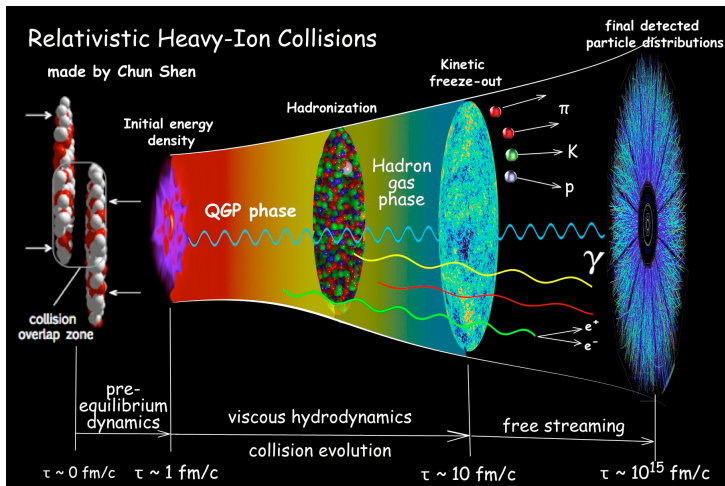
Bulk Properties

Summary of macroscopic characteristics of fireball

- **Temperature:** 100 – 500 MeV.
- **Volume:** $1 - 5 \times 10^3 \text{ fm}^3$.
- **Lifetime:** 10 – 20 fm/c.
- **Pressure:** 100 – 300 MeV/fm³.
- **Density:** $1 - 10 \rho_0$ ($\rho_0 = 0.17 \text{ fm}^{-3}$ normal nuclear density).

These properties are extracted from observables optimized to probe evolution of the system during the different stages of the collision.

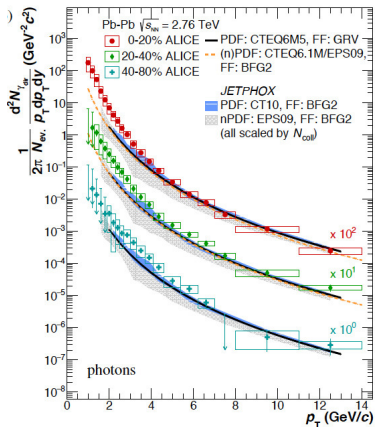
Collision evolution and observables



Evolution summary

- Initially, dense gluon fields create a strongly interacting medium. Initial state described by the Color Glass Condensate.
- Medium rapidly expands and thermalizes.
- QGP continues to expand and eventually cools down below $T_c \simeq 155$ MeV where it hadronizes and becomes a hadron-resonance gas.
- At a very similar temperature (known as chemical freeze-out temperature T^{chem}), particle composition is fixed.
- After chemical freeze-out, particles continue to interact. Only their momentum distributions are affected since their energy is below the inelastic reaction threshold.
- Hadrons cease to interact at a kinetic freeze out temperature $T^{\text{kin}} \simeq 95$ MeV, instant when they have developed a radial flow velocity $\langle\beta_T\rangle \simeq 0.65$.

Temperature from photon p_T distribution

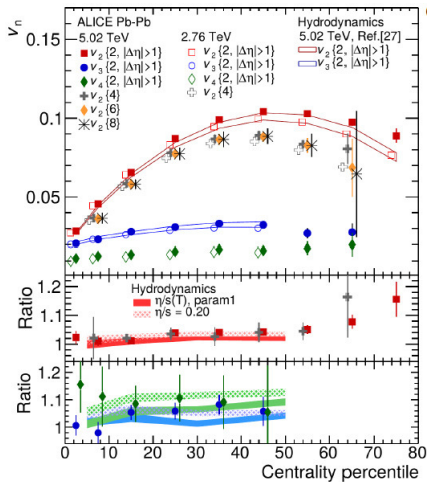


Photons shine through the QGP unaffected by strong interactions.
Inverse slope at low p_T gives $T_{\text{eff}} \simeq 300 \text{ MeV}$.

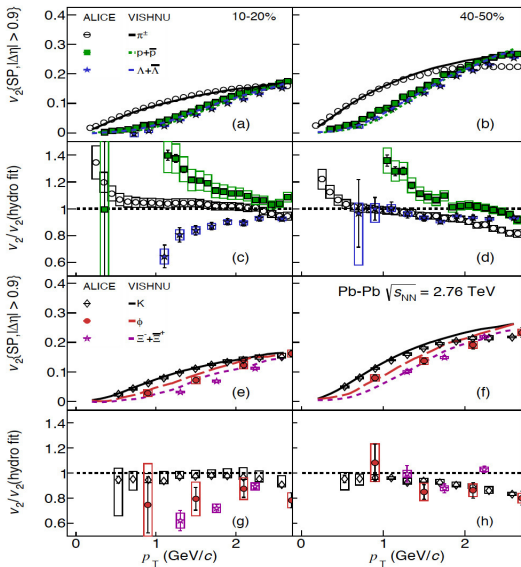
Hydrodynamics provides good description of bulk properties

- At low $p_T < 2$ GeV/c, **bulk matter dynamics is well described by relativistic hydrodynamical models.**
- A large fraction of all particles is produced in this p_T regime.
- The produced bulk medium behaves like an **almost perfect fluid** with a value of shear viscosity to entropy ration η/s close to its lower theoretical value.
- At a very similar temperature (known as chemical freeze-out temperature T^{chem}), particle composition is fixed.
- The medium is opaque to hard probes, quenching their energy.

$v_2(N_{\text{part}})$ vs. hydro models



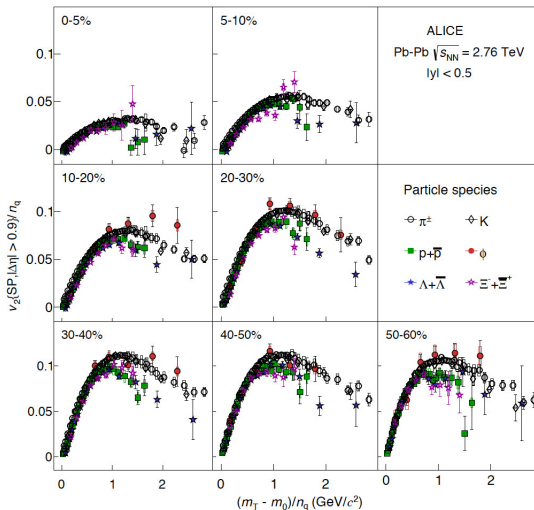
$v_2(p_T)$ vs. hydro models



Mass ordering

- Interplay between elliptic and radial flow.
- Radial flow tends to deplete the particle spectrum at low values (blue shift), which increases with increasing particle mass and transverse velocity.
- When immersed in a system with azimuthal anisotropy, depletion becomes larger in-plane than out-of-plane, thereby **reducing** v_2 .
- **The net result is that at a fixed value of p_T heavier particles have smaller v_2 than lighter ones.**

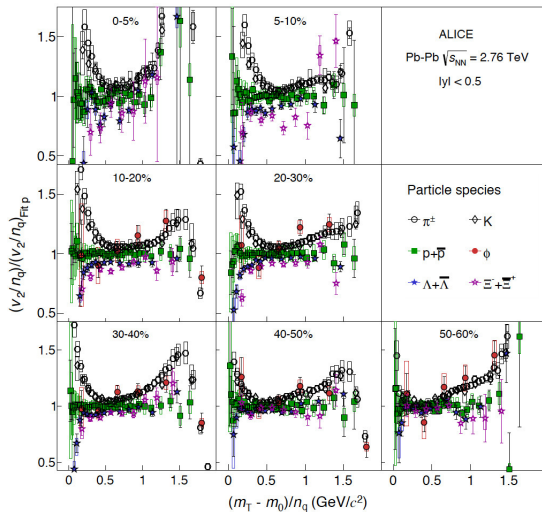
Scaling properties



Scaling properties

- At RHIC energies, it was reported that at intermediate p_T if **both** v_2 and p_T are scaled by the number of constituent quarks n_q , the various identified hadrons follow an approximate common behavior.
- To extend the scaling to lower p_T , v_2/n_q can be plotted as a function of the **transverse kinetic energy over the number of constituent quarks**
 $KE_T/n_q = (m_T - m_0)/n_q$, where $m_T = \sqrt{p_T^2 + m_0^2}$.
- Scaling was interpreted as **quark coalescence** being a dominant hadronization mechanism in this momentum domain and of **quark degrees of freedom dominating the early stages of heavy-ion collisions, when collective flow develops.**
- However, **ALICE data shows that scaling, if any, is only approximate for all centrality intervals.**

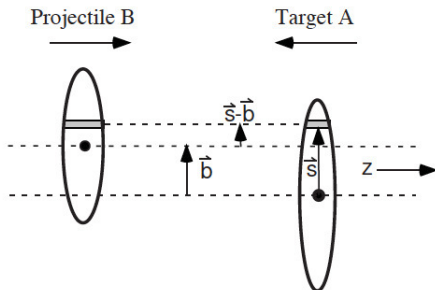
Deviations from scaling



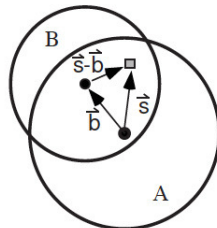
The systematic study of heavy-ion collisions requires experimental control parameters

- Collision energy per nucleon $\sqrt{s_{NN}}$, that can be varied by changing the beam energy.
- Overlap area of colliding nuclei, or alternatively **collision centrality**, usually given as a percentage of the geometrical cross section. Alternatively, one can provide the **number of participants in the collision**.
- N_{part} is estimated as an average over a given centrality range using a model describing the geometry of the collisions, so called **Glauber model**.

Glauber model

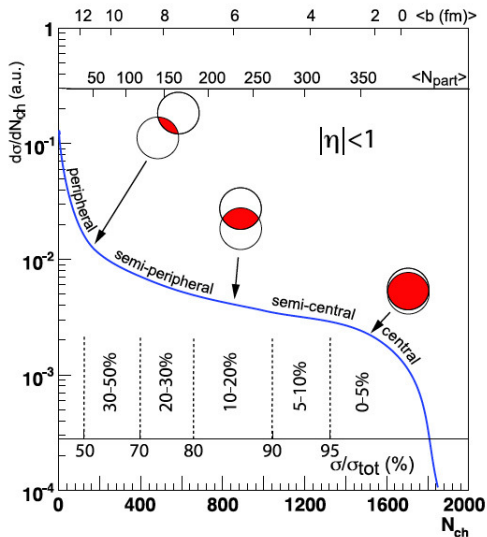


a) Side View

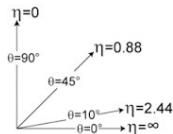


b) Beam-line View

Glauber model



Rapidity and pseudorapidity

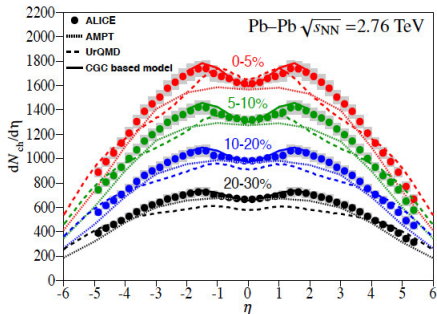
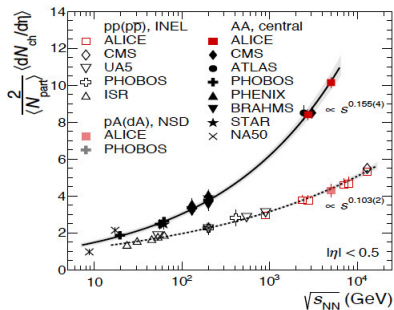


$$y = \frac{1}{2} \ln \left(\frac{E + p_z}{E - p_z} \right)$$

In the ultra-relativistic limit $m \sim 0$, $E \sim p$ and

$$\begin{aligned} y &\longrightarrow \frac{1}{2} \ln \left(\frac{1 + p_z/p}{1 - p_z/p} \right) \quad (\text{exercise}) \\ &= \frac{1}{2} \ln \left(\frac{\frac{1}{2} \cos^2(\theta/2)}{\frac{1}{2} \sin^2(\theta/2)} \right) \quad \theta \text{ is the polar angle} \\ &= -\ln \left(\tan \frac{\theta}{2} \right) \equiv \eta \end{aligned}$$

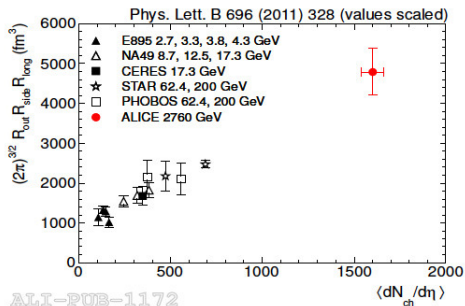
Multiplicity at $\sqrt{s_{NN}} = 2.76$ TeV, Pb+Pb



$$N_{ch} = 17,175 \pm 772 \quad 0 - 5\% \text{ centrality}$$

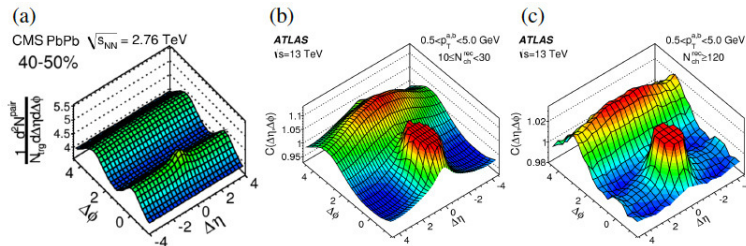
$$\frac{dN_{ch}}{d\eta} = 1,601 \pm 60 \quad |\eta| < 0.5$$

Size and life-time



Hanbury-Brown Twiss correlations indicate that for Pb+Pb collisions at $\sqrt{s_{NN}} = 2.76$ TeV the “**homogeneity volume**” (when strong interactions cease) is of about 5000 fm^3 , about twice as large of the one measured at RHIC. The decoupling time is about $10 \text{ fm}/c$, 30% larger than at RHIC.

Angular correlations



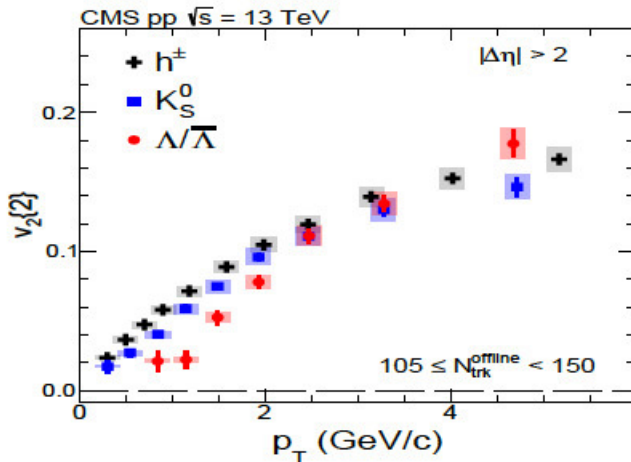
$\Delta\eta\Delta\phi$ distributions contain two important features:

- (1) A peak around $(\Delta\eta, \Delta\phi) = (0, 0)$ (near side peak from jets)
- (2) Long-range correlations called **ridges** (collective phenomena).

Similar structures observed in “**small reference systems**”.

Main possible explanations: Hydrodynamics and/or gluon saturation of the initial state (CGC).

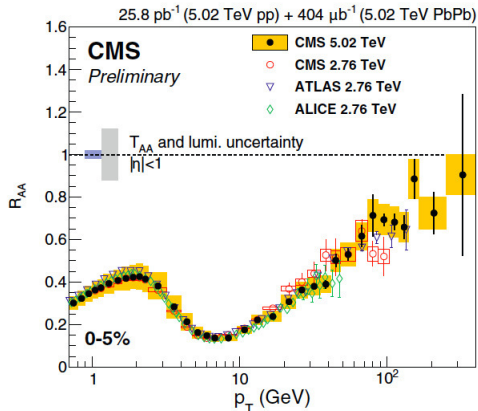
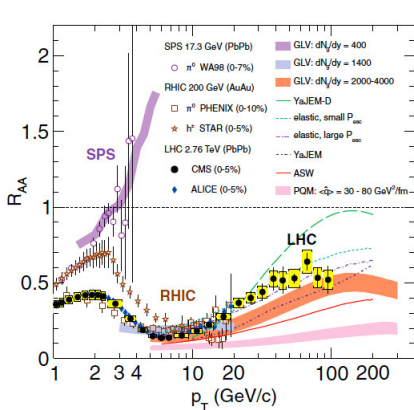
$v_2(p_T)$ in high multiplicity p+p events at $\sqrt{s} = 13$ TeV.



Hard Probes

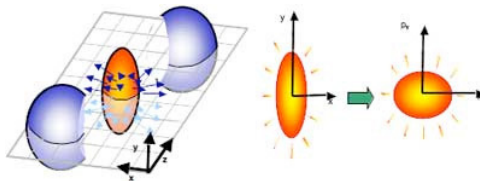
Energy loss

$$R_{AA}(p_T) = \frac{dN^{AA}(p_T)/p_T}{\langle N_{col} \rangle dN^{pp}(p_T)/p_T}$$



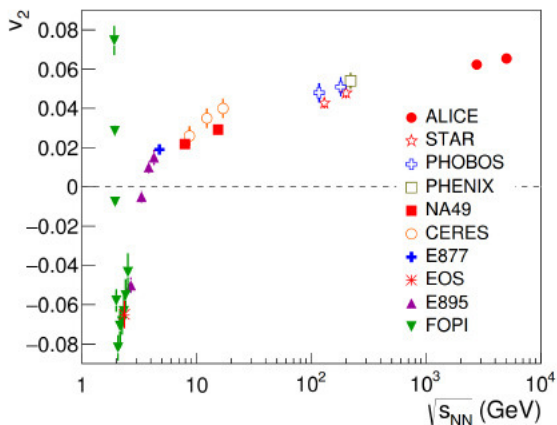
Elliptic flow

$$\frac{dN}{d(\phi - \Psi_R)} = N_0 [1 + 2v_1(p_T) \cos(\phi - \Psi_R) + 2v_2(p_T) \cos(2(\phi - \Psi_R)) \dots]$$

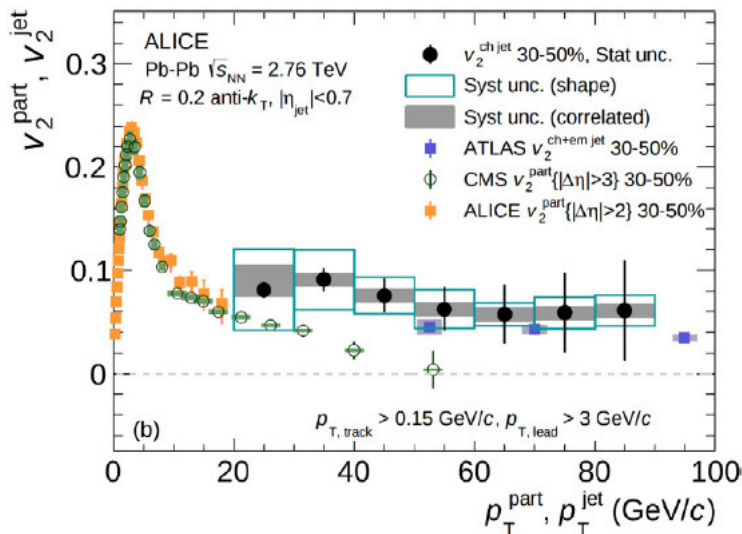


$\cos(2(\phi - \Psi_R))$ maximum for $(\phi - \Psi_R) = 0, \pi$,
 $dN/d(\phi - \Psi_R)$ maximum for $(\phi - \Psi_R) = 0, \pi$ provided $v_2(p_T) > 0$

Elliptic flow



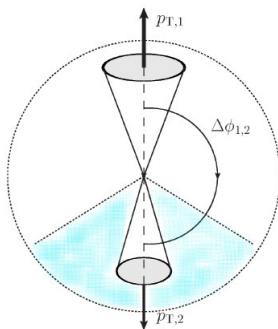
Elliptic flow



Energy loss connected to elliptic flow

- A significant positive $v_2^{\text{ch jet}}$ is observed in semi-central collisions.
- No significant p_T dependence can be observed.
- **Clear relationship between jet suppression (R_{AA}) and initial nuclear geometry (v_2).**
- The relationship confirms not only the existence of the medium but also the expectation that **jet suppression is strongest in the out-of-plane direction** where partons traverse the largest amount of hot matter.

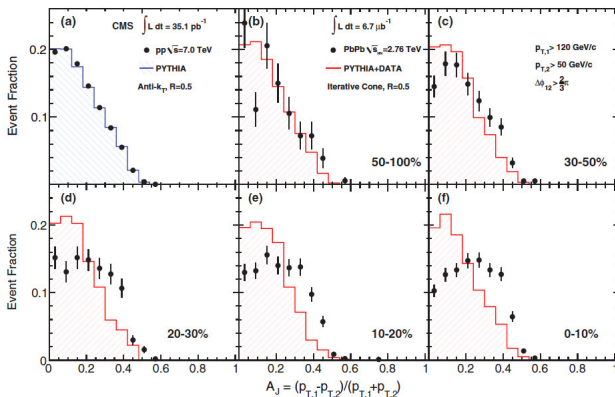
Where does the quenched jet energy go?



- 1 is the leading jet, 2 is the sub-leading jet.

Where does the quenched jet energy go?

- Asymmetry distribution as a function of $A_J = \frac{P_{T,1} - P_{T,2}}{P_{T,1} + P_{T,2}}$

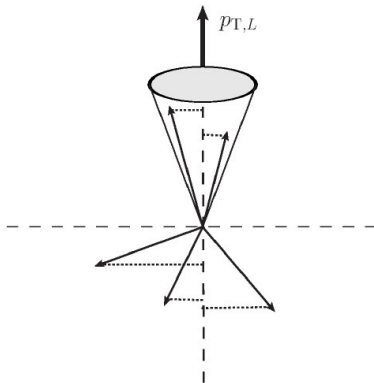


S. Chatrchyan et al. (CMS Collaboration), Phys. Rev. C **84**, 024906 (2011).

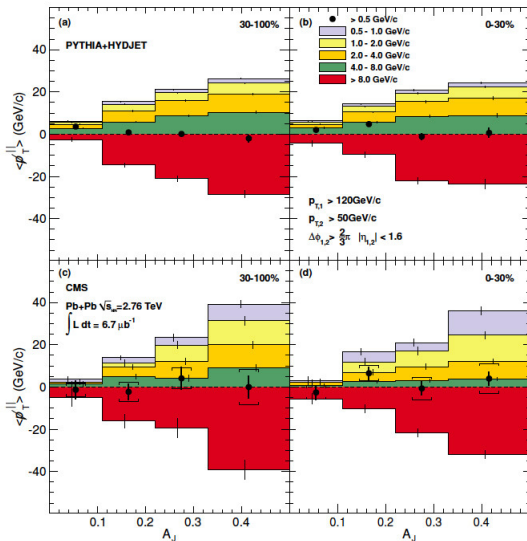
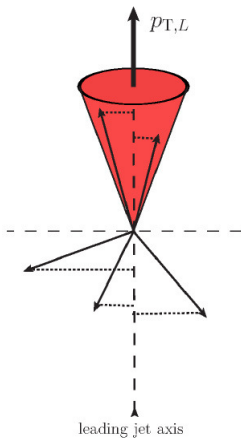
Missing p_T

- To quantify the amount of missing momentum inside away jet, define **average missing p_T**

$$\langle p_T^{\parallel} \rangle \equiv \frac{1}{N} \sum_{i \in \text{all } N \text{ tracks}} -p_T^i \cos(\phi_i - \phi_L)$$



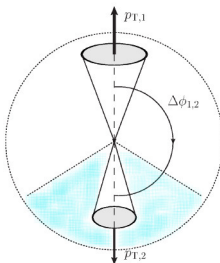
Missing p_T



S. Chatrchyan et al. (CMS Collaboration), Phys. Rev. C **84**, 024906

Missing p_T

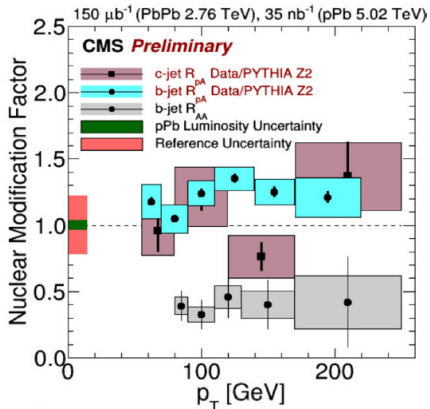
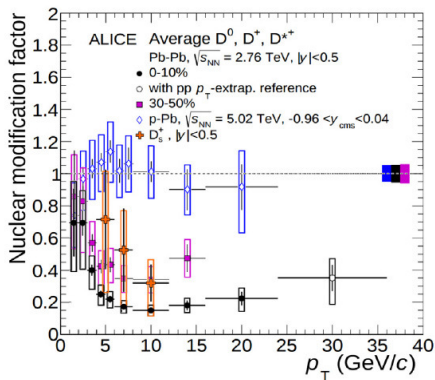
- The momentum in the away-side is obtained for tracks around the sub-leading jet **within a cone aperture larger than the jet cone.**
- Data show that the contribution to **the momentum around the leading cone comes mostly from tracks with $p_T > 8$ GeV.**
- **This momentum is balanced by the combined contributions from of tracks with $0.5 < p_T < 8$ GeV outside the away-side jet cone with $\Delta\phi < \pi/6$.**



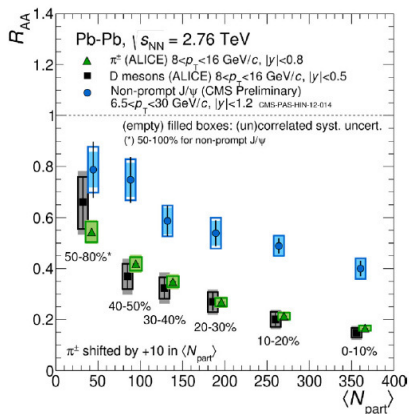
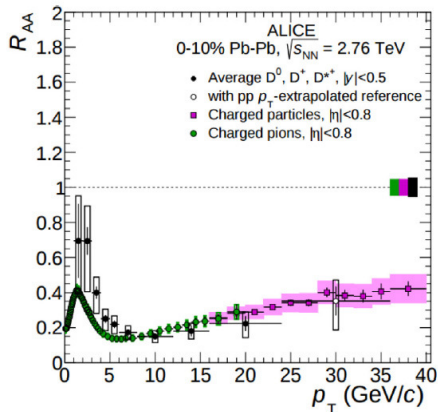
Heavy flavors

- Heavy flavors are produced by initial hard-scattering processes at time scales of order $\tau \sim 1/2m_H$ (0.07 fm for charm and 0.02 fm for bottom).
- These times are short compared to QGP formation ($\tau_0 \sim 0.1 - 1$ fm).
- Heavy flavors witness the entire medium evolution.
- Their annihilation rate in the QGP is small. Interaction with the medium may redistribute their momentum. This makes them a good probe for medium properties (transport coefficients).
- At the LHC, the production cross section is much larger than at RHIC, thus heavy flavors can be studied more systematically.

Heavy flavor open charm R_{AA}



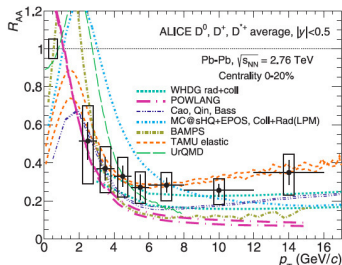
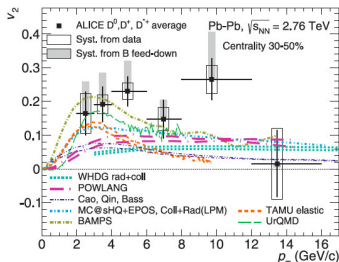
Heavy flavor open charm R_{AA}



Heavy flavor open charm R_{AA}

- Pure energy loss predicts $R_{AA}^{\text{light}} < R_{AA}^D < R_{AA}^B$ (hierarchy of suppression).
- **Caveat: There are a number of effects that alter such suppression pattern: Differences between primordial spectral shapes of produced partons and their fragmentation functions, differences between kinds of processes of flavor production (lights are mainly produced by soft processes, whereas heavies are produced by hard processes).**
- The observed agreement $R_{AA}(D) \simeq R_{AA}(\pi)$ is **reproduced by models that include different fragmentation functions and shapes of the primordial p_T distributions, in addition to the expected energy loss hierarchy.**
- Comparison of $R_{AA}(D)$ and $R_{AA}(J/\psi)$ shows the expected suppression pattern.

Heavy flavor elliptic flow



- Large energy loss indicates strong heavy-flavor coupling with medium
- Heavy-flavor hadrons can share the medium azimuthal anisotropy quantified by v_2 .
- Data show large v_2 of charm (same magnitude as v_2 of light-hadrons)
 \Rightarrow **charm thermalizes in medium.**
- Simultaneous measurements of R_{AA} and v_2 disentangles the interplay of different energy loss scenarios and imposes constraints on theoretical models.

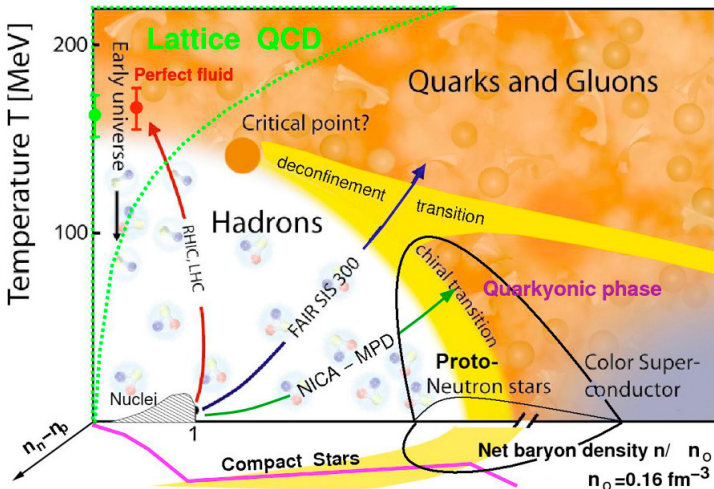
The phase diagram: QCD at finite T and μ_B .

- Two important parameters for QCD in equilibrium: The **temperature** T and the **baryon number density** n_B (or its conjugate variable $\mu_B = 3\mu_q$).

Since the intrinsic scale of QCD is $\Lambda_{\text{QCD}} \sim 200$ MeV, one expects a transition around $T \sim 200$ MeV, $n_B \sim \Lambda_{\text{QCD}}^3 \sim 1 \text{ fm}^{-3}$.

- Exploration of a wider range of the phase diagram with n_B up to several times the normal nuclear matter density $n_0 \sim 0.16 \text{ fm}^{-3}$ can be carried out by the BES-RHIC and other facilities such as FAIR at GSI, NICA at JINR, J-PARC at JAEA and KEK.
- In nature, the interior of compact stellar objects is the relevant system where dense and low temperature QCD matter is realized.

The phase diagram: QCD at finite T and μ_B .



Hadron thermodynamics

- Consider an ideal gas of identical neutral scalar particles of mass m_0 contained in a box volume V . Assume Boltzmann statistics. The partition function is given by

$$\mathcal{Z}(T, V) = \sum_N \frac{1}{N!} \left[\frac{V}{(2\pi)^3} \int d^3p \exp \left\{ -\frac{\sqrt{p^2 + m^2}}{T} \right\} \right]^N$$

$$\ln \mathcal{Z}(T, V) = \frac{VTm_0^2}{2\pi^2} K_2(m_0/T)$$

$$\epsilon(T) = -\frac{1}{V} \frac{\partial \ln \mathcal{Z}(T, V)}{\partial (1/T)} \xrightarrow{T \gg m_0} \frac{3}{\pi^2} T^4 \quad \text{energy density}$$

$$n(T) = -\frac{1}{V} \frac{\partial \ln \mathcal{Z}(T, V)}{\partial (V)} \xrightarrow{T \gg m_0} \frac{1}{\pi^2} T^3 \quad \text{particle density}$$

$$\omega(T) = \epsilon(T)/n(T) \simeq 3T \quad \text{average energy per particle}$$

An increase of system's energy has **three consequences**:

- A higher temperature
- More constituents
- More energetic constituents

Hadron thermodynamics

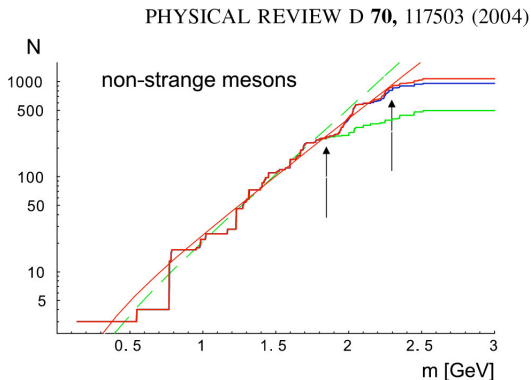
- Consider an ideal gas of hadrons that include **resonances**. The partition function is given by

$$\ln \mathcal{Z}(T, V) = \sum_i \frac{VTm_i^2}{2\pi^2} \rho(m_i) K_2(m_0/T)$$

- i starts with the ground state (m_0) and then includes the possible resonances with masses m_i .
- $\rho(m_i)$ is the weight corresponding to the state m_i .

Crucial point is to determine $\rho(m_i)$, i.e. **how many states are of mass m_i ?**

Hadron mass spectrum



$$\rho(m) \propto \exp \left\{ m/T^H \right\}, \text{ where } T^H \simeq 0.19 \text{ GeV}$$

Limiting temperature

The exponential growth of the density of states should be balanced by the Boltzmann factor $\exp\{-m/T\}$

$$\exp\left\{\frac{m}{T^H} - \frac{m}{T}\right\}$$

such that when $T > T^H$, the integration over m becomes singular. T^H plays the role of a limiting temperature (**Hagedorn Temperature**) above which the hadronic description breaks down.

Apply the argument to estimate the critical line at finite μ_B . The density of baryon states $\rho(m_B) \propto \exp\{m_B/T_B^H\}$ is balanced by the Boltzmann factor $\exp\{-(m_B - \mu_B)/T\}$. The limiting temperature

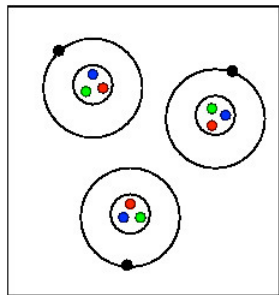
$$T = \left(1 - \frac{\mu_B}{m_B}\right) T_B^H.$$

Limiting temperature

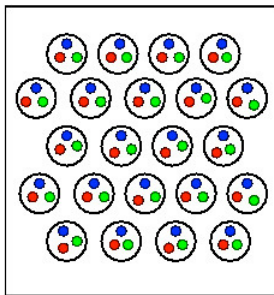
In contrast to the original analysis, the increase of energy leads to:

- A fixed temperature limit, $T \longrightarrow T^H$
- The momentum of the constituents do not continue to increase
- More and more species of ever heavier particles appear

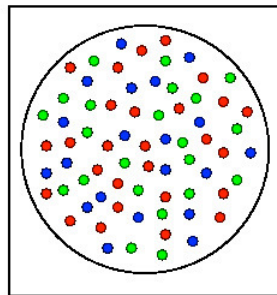
Percolation



(a)



(b)



(c)

Chiral symmetry restoration

- The QCD vacuum within hadrons should be regarded as a medium responsible for the non-perturbative quark mass.
- In hot and/or dense energetic matter quarks turn bare due to asymptotic freedom.
- **We expect a phase transition from a state with heavy constituent quarks to another with light current quarks.**
- The transition is called **chiral phase transition**.

Phase diagram from chiral symmetry restoration

- At finite T and μ the **QCD** phase diagram can also be studied from the point of view of chiral symmetry restoration.
- The order parameter is the **chiral condensate** $\langle\bar{\psi}\psi\rangle$. In vacuum $\langle\bar{\psi}\psi\rangle_0 = -(0.24 \text{ GeV})^3$. This value **sets the scale for the critical temperature of chiral restoration**.

In χ PT at low T and low n_B

$$\langle\bar{\psi}\psi\rangle_T / \langle\bar{\psi}\psi\rangle_0 = 1 - T^2/(8f_\pi^2) - T^4/(384f_\pi^4)$$

$$\langle\bar{\psi}\psi\rangle_{n_B} / \langle\bar{\psi}\psi\rangle_0 = 1 - \sigma_{\pi N} n_B / (f_\pi^2 m_\pi^2) - \dots$$

$$f_\pi \simeq 93 \text{ MeV, is the pion decay constant}$$

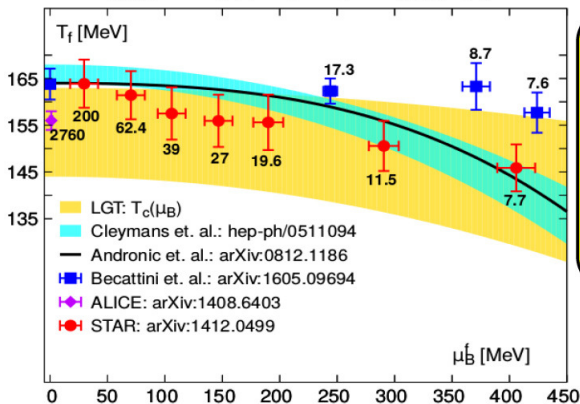
$$\sigma_{\pi N} = 40 \text{ MeV, is the } \pi - N \text{ sigma term}$$

- The result indicates that the **condensate melts at finite T and n_B** .

Chiral transition and hadronization

Chiral transition, hadronization and freeze-out

$$\text{LGT: } T_c(\mu_B) = 154(9)(1 - [0.006; 0.014](\mu_B/T)^2)\text{MeV}$$



phenomenological freeze-out / hadronization curve, QCD transition line and experimental data (obtained by assuming the validity of the HRG model) are consistent for

$$\mu_B/T \lesssim 3$$

HOWEVER

physics is quite different at lower and upper end of the current error bar on T_c



probed with net-charge correlations&fluctuations

Chiral transition and hadronization

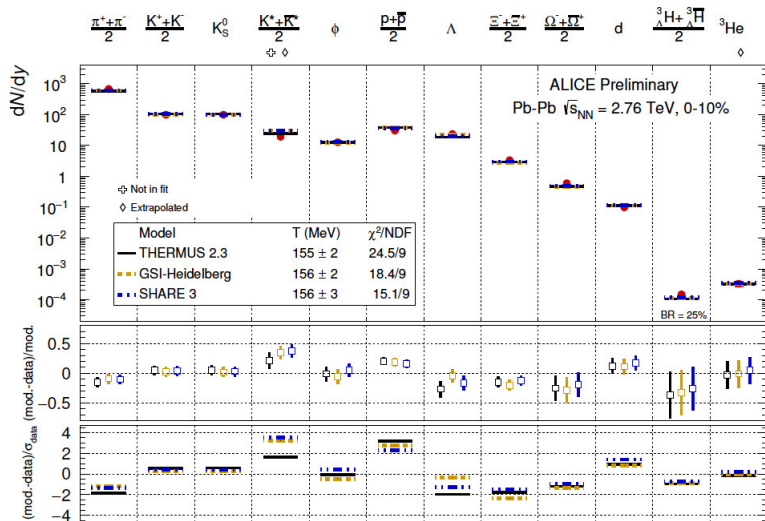
- Hadron multiplicities established very close to the phase boundary.

Statistical model

$$n_j = \frac{g_j}{2\pi^2} \int_0^\infty p^2 dp \left[\exp \left\{ \sqrt{p^2 + M_j^2} / T_{\text{ch}} - \mu_{\text{ch}} \right\} \pm 1 \right]^{-1}$$

- From the hadron side, abundances due to multi-particle collisions whose importance is **enhanced due to high particle density in the phase transition region**. **Collective phenomena play an important role.**
- **Since the multi-particle scattering rates fall-off rapidly, the experimentally determined chemical freeze-out is a good measure of the phase transition temperature.**

Statistical model and particle ratios



ALI-PREL-94600

Phase transitions

What is a phase transition?

- Transformation of a given substance from one state of matter to another.
- During the phase transition some quantities change, often in a discontinuous manner.
- Changes result in variations of external conditions such as pressure, temperature, etc.



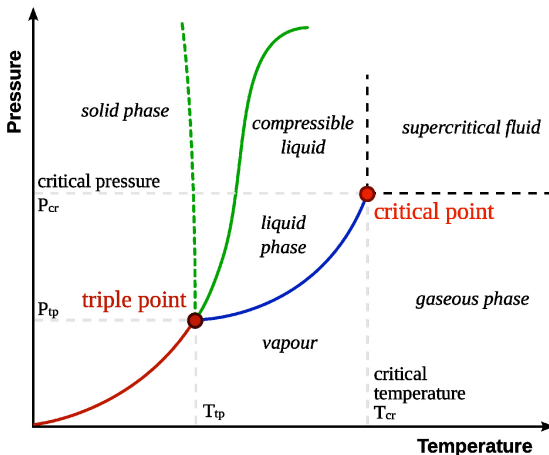
Phase transitions

When does a phase transition happen?

- In technical terms, they occur when the **free energy is non-analytic (one of its derivatives diverges)** for some values of the thermodynamical variables.
- They result from the interaction of a **large number of particles** and in general it does not occur when the system is very small or has a small number of particles.
- On the phase transition lines **the free energies in one and the other phase coincide.**
- Some times it is possible to change the state of a substance without crossing a phase transition line. Under these conditions one talks about a **crossover transition.**

Phase transitions

Characteristics of a phase diagram



Phase transitions

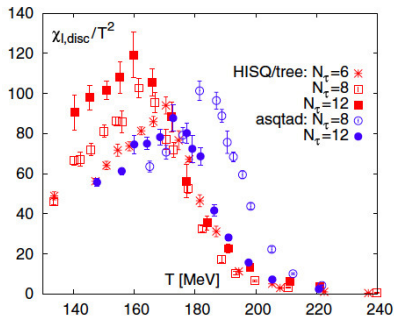
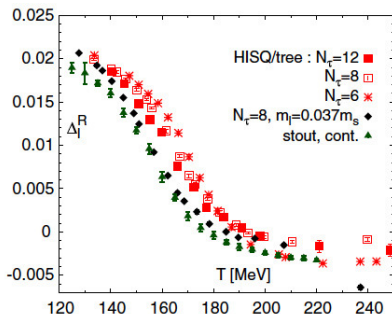
Classification, according to behavior of free energy as a function of a given thermodynamical variable (Ehrenfest). **They are named according to the derivative of lowest order that becomes discontinuous during the transition**

- **First order:** First derivative of free energy is discontinuous. **Example: boiling water.** Discontinuity in the density, i.e. derivative of free energy with respect to chemical potential.
- **Second order:** First derivative is continuous. Second derivative is discontinuous. **Example: Ferromagnetism.** The magnetization, i.e. the derivative of the free energy with respect to the external field is continuous. The susceptibility, i.e. the derivative of the magnetization with respect to the external field, is discontinuous.

Modern classification

- **First order:** Involve **latent heat**. System absorbs or releases heat at a constant temperature. Phases coexist. Some parts have completed the transition and some others haven't.
- **Second order:** They are **continuous** transitions. Susceptibilities diverge, correlation lengths become large.

Lattice QCD at finite T



A. Bazavov *et al.*, Phys. Rev. D **85**, 054503 (2012).

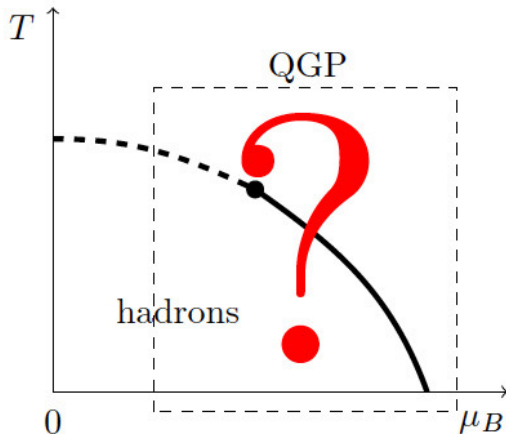
Transition features ($\mu = 0$)

- It is an analytic (there are no divergences in thermodynamic quantities) **crossover** for $\mu = 0$. There are no symmetries to break. It would be a real phase transition for massless quarks.
- It is believed that the first order phase transition turns into a second order phase transition somewhere in the middle of the phase diagram.

Critical temperature from lattice QCD for $\mu = 0$

- T_c from the susceptibility's peak for 2+1 flavors using different kinds of fermion representations.
- Values show some discrepancies:
- The MILC collaboration obtains $T_c = 169(12)(4)$ MeV.
- The BNL-RBC-Bielefeld collaboration reports $T_c = 192(7)(4)$ MeV.
- The Wuppertal-Budapest collaboration has consistently obtained smaller values, the last being $T_c = 147(2)(3)$ MeV.
- The HotQCD collaboration has reported $T_c = 154(9)$ MeV.
- Differences may be attributed to different lattice spacings.

For $\mu \neq 0$ matters get complicated: Sign problem



The sign problem

- Lattice QCD is affected by the **sign problem**
- The calculation of the partition function produces a fermion determinant.

$$\text{Det}M = \text{Det}(\not{D} + m + \mu\gamma_0)$$

- Consider a complex value for μ . Take the determinant on both sides of the identity

$$\gamma_5(\not{D} + m + \mu\gamma_0)\gamma_5 = (\not{D} + m - \mu^*\gamma_0)^\dagger,$$

we obtain

$$\text{Det}(\not{D} + m + \mu\gamma_0) = [\text{Det}(\not{D} + m - \mu^*\gamma_0)]^*,$$

- This shows that **the determinant is not real unless $\mu = 0$ or purely imaginary.**

The sign problem

- For **real** μ it is not possible to carry out the direct sampling on a finite density ensemble by Monte Carlo methods
- It'd seem that the problem is not so bad since we could naively write

$$\text{Det}M = |\text{Det}M|e^{i\theta}$$

- To compute the thermal average of an observable O we write

$$\langle O \rangle = \frac{\int DU e^{-S_{YM}} \text{Det}M O}{\int DU e^{-S_{YM}} \text{Det}M} = \frac{\int DU e^{-S_{YM}} |\text{Det}M| e^{i\theta} O}{\int DU e^{-S_{YM}} |\text{Det}M| e^{i\theta}},$$

- S_{YM} is the Yang-Mills action.

The sign problem

- Note that written in this way, the simulations can be made in terms of the *phase quenched theory* where the measure involves $|\text{Det}M|$ and the thermal average can be written as

$$\langle O \rangle = \frac{\langle O e^{i\theta} \rangle_{\text{pq}}}{\langle e^{i\theta} \rangle_{\text{pq}}}.$$

- The average phase factor (also called the average sign) in the **phase quenched theory** can be written as

$$\langle e^{i\theta} \rangle_{\text{pq}} = e^{-V(f - f_{\text{pq}})/T},$$

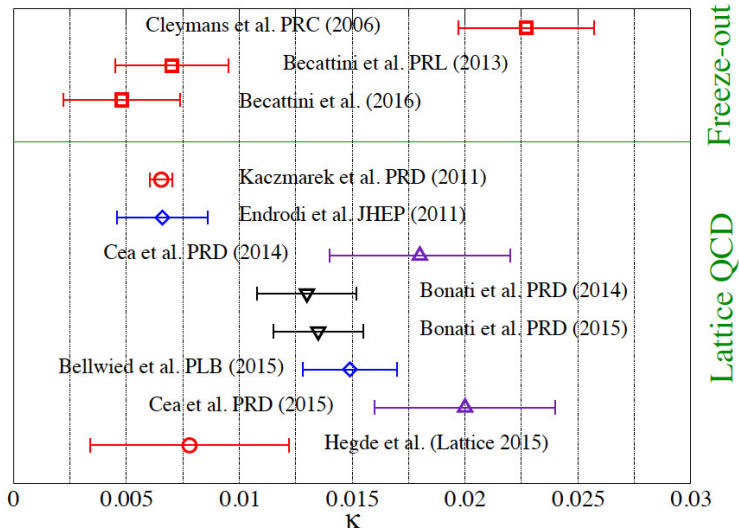
where f y f_{pq} are the free energy densities of the full and the phase quenched theories, respectively and V is the 3-dimensional volume.

- If $f - f_{\text{pq}} \neq 0$, the average phase factor decreases exponentially when V grows (thermodynamical limit) and/or when T goes to zero.
- Under these circumstances the signal/noise ratio worsens. **This is known as the severe sign problem.**

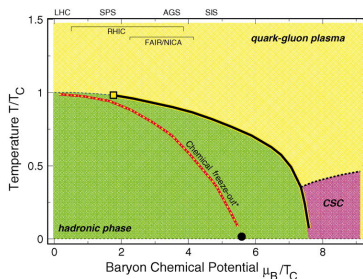
Curvature of freeze-out / transition curve $\mu = 0$

- In lattice QCD it is possible to make a Taylor expansion for small μ .
- The expansion coefficients can be expressed as the expectation values of traces of polynomial matrices taken on the ensemble with $\mu = 0$.
- Although care has to be taken with the growing of the statistical error, this strategy gives rise to an important result: The **curvature κ of the transition curve** para $\mu = 0$.
- Values for $\kappa=0.006-0.02$ have been reported.
- Latest determination of κ similar to curvature for **chemical freeze-out** curve.

Curvature of freeze-out / transition curve $\mu = 0$



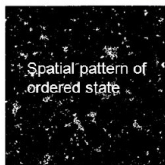
Is there a Critical End Point?



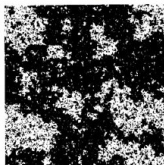
- Most of the **effective models** suggest the existence of a **QCD** critical point (μ_{CEP} , T_{CEP}) somewhere in the middle of the phase diagram **where the crossover line becomes a first order transition line.**
- Signals are and will be looked for in current and future facilities.

Critical point and critical phenomena

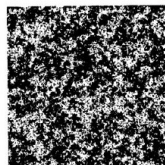
Ordered $T=0.995T_c$



Critical $T=T_c$



Disordered $T=1.05T_c$



2D-Ising model simulation from ISBN4-563-02435-X C33421

Critical Phenomena :

- Density fluctuations and cluster formations.
- Divergence of Correlation length (ξ).
- Susceptibilities (χ), heat capacity (C_V), Compressibility (κ) etc.
- Critical opalescence.
- Universality and critical exponents determined by the symmetry and dimensions of underlying system.

First CP is discovered in 1869 for CO_2

$$T_c = 31^\circ\text{C}$$

Can we discovery the Critical Point of Quark Matter ? (Put a permanent mark in the QCD phase diagram in text book.)

$$T_c \sim \text{Trillion } (10^{12})^\circ\text{C}$$

Analysis tool: Fluctuations of conserved quantities

- Thermodynamics, fundamental object partition function \mathcal{Z} , is also de *moment generating function*.
- Work with $\ln \mathcal{Z}$, also known as the *cumulant generating function*.
- The first cumulant is the expectation value; the second and third cumulants are respectively the second and third *central moments*. The fourth cumulant is related to the **kurtosis**.
- Experimentally easy to measure the central moments M :
$$M_{BQS}^{ijk} = \langle (B - \langle B \rangle)^i (Q - \langle Q \rangle)^j (S - \langle S \rangle)^k \rangle.$$
- On the other hand, derivatives of $\ln \mathcal{Z}$ with respect to the *chemical potentials* give the *susceptibilities* χ :

$$\chi_{BQS}^{ijk} = \frac{\partial^{i+k+j}(P/T^4)}{\partial^i(\mu_B/T) \partial^j(\mu_Q/T) \partial^k(\mu_S/T)}; \quad P = \frac{T}{V} \ln \mathcal{Z}.$$

$$\Rightarrow \chi_{XY} = \frac{1}{V} T^3 M_{XY}^{11}$$

Fluctuations of conserved quantities

1. Higher sensitivity to correlation length (ξ) and probe non-gaussian fluctuations.

$$C_{1,x} = \langle x \rangle, C_{2,x} = \langle (\delta x)^2 \rangle,$$

$$C_{3,x} = \langle (\delta x)^3 \rangle, C_{4,x} = \langle (\delta x)^4 \rangle - 3 \langle (\delta x)^2 \rangle^2$$

$$\langle (\delta N)^3 \rangle_c \approx \xi^{4.5}, \quad \langle (\delta N)^4 \rangle_c \approx \xi^7$$

M. A. Stephanov, *Phys. Rev. Lett.* 102, 032301 (2009).

M. A. Stephanov, *Phys. Rev. Lett.* 107, 052301 (2011).

M. Asakawa, S. Ejiri and M. Kitazawa, *Phys. Rev. Lett.* 103, 262301 (2009).

Y. Hatta, M. Stephanov, *Phys. Rev. Lett.* 91, 102003 (2003).

2. Connection to the susceptibility of the system.

$$\frac{\chi_q^4}{\chi_q^2} = \kappa \sigma^2 = \frac{C_{4,q}}{C_{2,q}}, \quad \frac{\chi_q^3}{\chi_q^2} = S \sigma = \frac{C_{3,q}}{C_{2,q}},$$

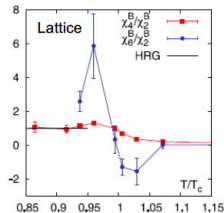
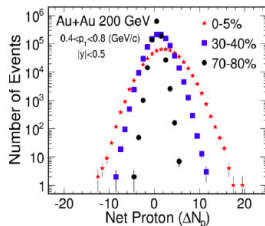
$$\chi_q^{(n)} = \frac{1}{VT^3} \times C_{n,q} = \frac{\partial^n (p/T^4)}{\partial (\mu_q)^n}, q = B, Q, S$$

S. Ejiri et al, *Phys. Lett. B* 633 (2006) 275. Cheng et al, *PRD* (2009) 074505. B.

Friman et al., *EPJC* 71 (2011) 1694. F. Karsch and K. Redlich, *PLB* 695, 136 (2011).

S. Gupta, et al., *Science*, 332, 1525(2012). A. Bazavov et al., *PRL* 109, 192302(12) // S.

Borsanyi et al., *PRL* 111, 062005(13) // P. Alba et al., *arXiv:1403.4903*



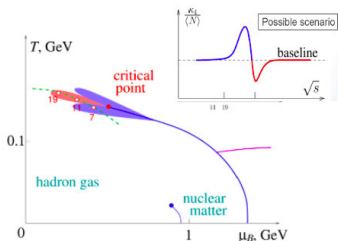
Higher moments, larger sensitivity to correlation length ξ

- In HIC's, the simplest measurements of fluctuations are event-by-event variances in observables such as multiplicities or mean transverse momenta of particles.
- At the CEP, these variances diverge approximately as ξ^2 . **They manifest as a non-monotonic behavior as the CEP is passed by during a beam energy scan.**
- In a realistic HIC, the divergence of ξ is tamed by the effects of *critical slow down* (the phenomenon describing a finite and possibly large relaxation time near criticality).
- However, higher, non-Gaussian moments of the fluctuations depend much more sensitively on ξ .
- **Important to look at the Kurtosis κ (proportional to the fourth-order cumulant C_4), which grows as ξ^7 .**

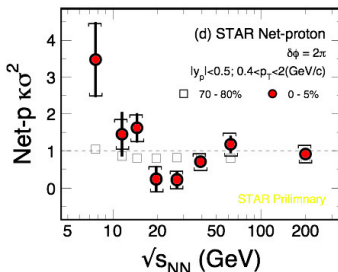
Fourth order fluctuations: Net proton

$$K\sigma^2 = C_4/C_2$$

Model



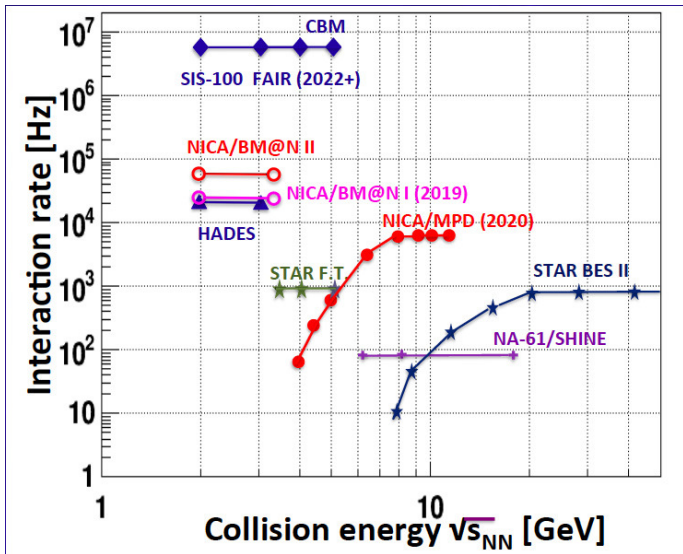
STAR BES Data



M.A. Stephanov, PRL107, 052301 (2011).
 Schaefer&Wanger, PRD 85, 034027 (2012)
 Vovchenko et al., PRC92, 054901 (2015)
 JW Chen et al., PRD93, 034037 (2016)
 arXiv: 1603.05198.

Non-monotonic energy dependence is observed for 4th order net-proton fluctuations in most central Au+Au collisions.

Dedicated experiments to explore QCD phase diagram



Summary and open questions

- **Heavy-Ion Standard Model** is being developed. Synergy of experiment and theory. Experimental measurements pose many theoretical challenges and rise questions stimulating progress.
- **Diversity of approaches:** Semiclassical gauge theory for initial conditions. LQCD for static thermodynamic properties. Perturbative QCD in vacuum and in-medium. Transport theory and particularly viscous hydrodynamics for the evolution of bulk matter. Even holographic methods can be employed to describe the dynamics of thermalization.
- **Variety of open problems in different fronts:** Thermal photon puzzle, extraction of transport coefficients, interplay between hard and soft modes, limit of applicability of hydro approach and inclusion of bulk viscosity in 3D calculations, role of magnetic fields in peripheral collisions, critical point of phase diagram...
- **Exciting field with many opportunities to continue exploring the properties of QCD matter under extreme conditions.**